Ab initio investigation of the CO-N2 quantum scattering: The collisional perturbation of the pure rotational R(0) line in CO

H. Jóźwiak, Franck Thibault, H. Cybulski, P. Wcislo

Ab initio investigation of the CO-N_2 quantum scattering: the collisional perturbation of the pure rotational R(0) line in CO

Hubert Jóźwiak,[1, a)] Franck Thibault,[2] Hubert Cybulski,[3] and Piotr Wcisło[1, b)]
[1)]*Institute of Physics, Faculty of Physics, Astronomy and Informatics, Nicolaus Copernicus University, Grudziadzka 5, 87-100 Toruń, Poland*
[2)]*Univ Rennes, CNRS, IPR (Institut de Physique de Rennes)-UMR 6251, Rennes F-35000, France*
[3)]*Institute of Physics, Kazimierz Wielki University, ul. Powstańców Wielkopolskich 2, 85-090 Bydgoszcz, Poland*

(Dated: 14 January 2021)

We report fully quantum calculations of the collisional perturbation of a molecular line for a system that is relevant for Earth's atmosphere. We consider the N_2-perturbed pure rotational R(0) line in CO. The results agree well with the available experimental data. This work constitutes a significant step towards populating the spectroscopic databases with *ab initio* collisional line-shape parameters for atmosphere-relevant systems. The calculations were performed using three different recently reported potential energy surfaces (PESs). We conclude that all three PESs lead to practically the same values of the pressure broadening coefficients.

I. INTRODUCTION

Detailed knowledge about the interaction energy in molecular systems is crucial for understanding variety of physical phenomena. An accurate potential energy surface (PES) is important for the calculations of bound states of molecular complexes,[1] understanding the dynamics of the interstellar medium,[2] proper interpretation of collisionally induced spectra[3] and determination of shapes of the optical molecular resonances.[4] Nitrogen molecule, as the main constituent of Earth's atmosphere, is of particular importance for the spectroscopic community. Collisions with N_2 can perturb the absorption lines of less abundant molecules in the atmosphere, leading to the pressure broadening (and shift) of the spectra, and constitute the primary broadening mechanism in the troposphere.[5] Accurate values of pressure broadening and shift coefficients are essential for reducing atmospheric-spectra fit residuals,[6] which might affect values of the quantities retrieved from the fit, such as the volume mixing ratio (VMR)[6,7] of the absorbing compound. This is especially important in terms of remote sensing applications, as subpercent accuracy of the VMR is needed to reliably identify the sources and sinks of the greenhouse gases.[8,9] Carbon monoxide is a trace gas in Earth's atmosphere which has an indirect impact on the concentration of methane. Indeed, CO reacts with hydroxyl radicals (·OH) and reduces their abundance in the atmosphere, which, in turn, leads to higher concentration of the CH_4 molecules.[10,11] Carbon monoxide is also an important gaseous pollutant and a useful tracer of various anthropogenic activities, such as fossil fuel combustion.[12–14]

Apart from remote sensing measurements, accurate pressure broadening coefficients of the nitrogen-perturbed CO lines are of particular importance in the analysis of the atmospheres of various objects in the outer Solar System. The atmosphere of Titan, the largest moon of Saturn, is dominated by nitrogen (94.2%) and methane (5.65%).[15,16] Trace amounts of the CO molecule were discovered there by Lutz *et al.*,[17] who identified several P and R lines of the 3-0 band from ground-based measurements. To accurately determine the CO concentration in Titan's atmosphere, several studies were pursued, where pure rotational transitions,[18,19] in particular the R(0),[20–23] R(1),[23,24] R(2)[23,25] lines, as well as transitions from the fundamental band, were investigated.[26–28] Currently,[29] the most accurate values of the VMR of carbon monoxide come from ground-based measurements using the Submillimeter Array,[25] from the SPIRE instrument on the Herschel satellite,[30] and the Composite Infrared Spectrometer (CIRS) on board the Cassini probe[19] and are given by (5.1 $\pm$ 0.4) $\times 10^{-5}$, (4.0 $\pm$ 0.5) $\times 10^{-5}$ and (4.7 $\pm$ 0.8) $\times 10^{-5}$, respectively. In all these investigations, the experimental values[31–34] of the pressure broadening coefficients of the N_2-perturbed CO lines were necessary to properly interpret the measured spectra.

Carbon monoxide was also detected in the nitrogen-dominated[35] atmosphere of Triton, the largest moon of Neptune.[36] The ground-based spectroscopic observations of Triton in the 2.32-2.37 μm region, using the European Southern Observatory Very Large Telescope (ESO VLT), determined the abundance of CO and CH_4 to be at a level of a few hundredths of a percent of that of the nitrogen. Accurate information about the relative abundance of CO and CH_4 is especially needed for the analysis of seasonal changes of Triton's atmosphere[37] and could be a subject of interest for future orbital missions to Neptune.[38] The atmosphere of Pluto shares some similarities to those of Triton and Titan, as consists mostly of nitrogen, with trace amounts of methane (0.25%) and carbon monoxide.[39] Searches for the CO features in the atmospheric spectra of Pluto were subjects of various investigations in the millimeter[40–43] and near-IR ranges.[44,45] The analysis of the pure rotational R(2) line by Lellouch *et al.* indicated a CO mole fraction of 515 $\pm$ 40 ppm for a surface pressure of 12 μbars.[43]

[a)]Electronic mail: hubert.jozwiak@doktorant.umk.pl
[b)]Electronic mail: piotr.wcislo@umk.pl

As a molecular complex, the CO-N_2 system was a subject of thorough theoretical and experimental investigations throughout past years. The first pure rotational spectra of the CO-N_2 complex were observed in 1996[46,47] in the IR region. These works were followed by studies of the microwave and millimeter transitions in the complex,[48–52] and several studies devoted to the transitions in the IR region.[53,54] We recall also two very recent studies of this complex in the millimeter range,[55,56] which provided an accurate test of the recently reported PESs.[55,57,58]

The theoretical investigations on the CO-N_2 complex were reviewed in more detail in a previous paper.[57] Here, we only recall the importance of the study conducted by Fišer and Polák,[59] who investigated multiple orientations of the complex using the coupled-cluster singles and doubles including connected triple corrections [CCSD(T)] and Møller-Plesset (MP) perturbation theory up to fourth order. The first four-dimensional (4D) PES was reported by Karimi-Jafari *et al.*,[60] who employed the MP4 method with a basis set obtained from the Dunning's aug-cc-pVQZ basis set. In this investigation, the g and f functions were removed from the original basis set and, additionally, a set of 3s3p2d1f midbond functions was used. Nonetheless, as it was stated in Ref. 57, due to the method used, reduction of the basis set and too small number of grid points chosen by the authors, this PES should not be considered reliable enough to study various physical phenomena. Recently, three highly accurate PESs were reported.[55,57,58] Liu *et al.*[58] calculated a 5D PES using the CCSD(T)-F12 method and the aug-cc-pVQZ basis set, claiming the discrepancies between theoretical and experimental energies of the IR transitions of the CO-N_2 complex to be smaller than 0.068 cm^{-1}. Surin *et al.*[55] reported a 4D PES calculated using the standard CCSD(T) method and the aug-cc-pVQZ basis set, supplemented with 3s2p1d midbond functions. The accompanying experimental results enabled the authors to assign several newly detected transitions. However, some significant discrepancies between the calculated and experimental rotational states were observed. The third, more recent potential,[57] was calculated using the CCSD(T) method with the aug-cc-pVQZ basis set, extended with the 3s3p2d1f1g midbond functions. This 4D PES was fit to an analytical expression,[57] which performs well for geometries where the interaction energy does not exceed 100 μE_h. The agreement between the theoretical and experimental values of the energy levels is significantly better than for all the aforementioned PESs.

Collisional broadening of the CO lines by nitrogen molecules has been studied in detail both theoretically and experimentally. A majority of the experimental data refers to the lines in the fundamental band of CO.[33,34,61–89] N_2-perturbed CO lines were also measured for the first[84,90–94] and second overtones.[65,95–97] In the case of pure rotational transitions, the pressure broadening coefficients of the N_2-perturbed lines were determined for the first five R lines of CO. The first measurements of the nitrogen-, oxygen- and air-broadened widths of the R(0) line were reported by Connor and Radford,[98] and by Colmont and Monnanteuil.[31] These results were refined by Nissen *et al.*[99] in a comparative study of foreign gas pressure broadening of the R(0) line, using Fourier-transform and radio-acoustical detection spectrometers. There are also a few papers regarding foreign gas broadening of the R(1),[32] R(2)[100] and R(4)[101,102] CO lines, in which a temperature dependence of the N_2 broadening coefficients was determined. Puzzarini *et al.*[103] reported a thorough study of various line-shape models in the analysis of the N_2- and O_2-broadened R(0-3) lines at 296 K. The pressure broadening coefficients of the N_2-perturbed CO lines from the S branch were also determined using coherent anti-Stokes Raman scattering (CARS) spectroscopy.[104]

It has been recently shown for a benchmark system of helium-perturbed H_2, that a full *ab initio* description of the shapes of rovibrational transitions leads to subpercent agreement with experimentally measured spectra.[105] This successful theoretical approach is based on a very accurate PES, determined from first principles,[106,107] quantum scattering calculations and a state-of-the-art model of collision-perturbed shape of rovibrational resonance,[108–111] which includes the speed dependence of line broadening and shift[112] and the influence of velocity changing collisions.[113] Helium-perturbed H_2 lines were subjects of several recent investigations. In Ref. 114 the influence of PESs' quality on shapes of particular rovibrational lines was studied in detail. The most accurate PES for this system and line-shape parameters for the rovibrational Q lines were reported in Ref. 107. Shapes of optical resonances from the O and S branches were determined in Ref. 115. Importance of centrifugal distortion (the dependence of the radial coupling terms of the PES on the rotational quantum number) was studied in Ref. 116. Finally, the first comprehensive database of the line-shape parameters (broadening, shift, their speed dependence and the complex Dicke parameter), generated from *ab initio* calculations, was reported in Ref. 117. The same methodology was applied to the cases of helium-perturbed lines of HD[118,119] and D_2.[120,121] Recently, subpercent agreement with the experimental shapes of Ar-perturbed rovibrational lines in CO was achieved.[122]

Here, we report the *ab initio* quantum scattering calculations of the collision-perturbed shape of the molecular line for a system that is relevant for the terrestrial atmosphere. We investigate the width of the N_2-perturbed pure rotational R(0) line in CO. Scattering calculations are performed using three PESs.[55,57,58] Our results are in good agreement with the available experimental data.[31,98,99,103] The shape of the pure rotational R(0) line is dominated by the collisional broadening, which is two orders of magnitude larger than the pressure induced shift. Hence, in this paper we do not consider the pressure shift coefficient. Due to the complex structure of the close-coupled (CC) equations and a large number of channels that must be taken into account, the equations are solved using the coupled states approximation (CSA).[123]

The paper is organized as follows: in Sec. II we briefly describe the PESs used in the calculations. In Sec. III we discuss the details of the scattering calculations and we analyze the obtained generalized spectroscopic cross sections. In Sec. IV we describe the calculations of the pressure broadening coefficient and in Sec. V we compare our results with the experimental data. The accuracy of our calculations we discuss in

Sec. VI and in Sec. VII we summarize our results.

II. POTENTIAL ENERGY SURFACE

A PES for a system consisting of two rigid diatomic molecules (A and B) depends on four variables: the intermolecular distance between the centers of mass of the molecules, R, the angles between each of the molecular axes and the intermolecular axis, θ_A and θ_B, and the dihedral angle, ϕ. Let us identify subscripts A and B with CO and N_2 molecules, respectively. The definition of the angles is presented in Fig. 1. Contrary to the PESs of Surin *et al.*[55] and Cybulski *et al.*,[57] which are 4D, the PES of Liu *et al.*[58] additionally takes into account the stretching of the CO molecule. However, for the purpose of these calculations (we investigate a pure rotational transition in the ground vibrational state of CO), we do not consider any changes of the intramolecular distance of the molecule.

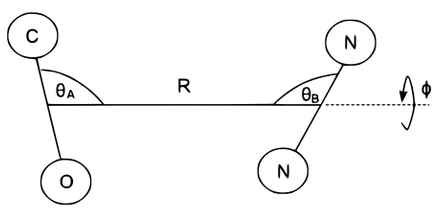

FIG. 1. Geometry of the CO-N_2 system.

In order to reduce the potential to a form suitable for the scattering calculations, the 4D PES is expanded over bispherical harmonics:

$$V(R,\theta_A,\theta_B,\phi) = \sum_{l_A,l_B,l} A_{l_A,l_B,l}(R) I_{l_A,l_B,l}(\theta_A,\theta_B,\phi). \quad (1)$$

The radial terms of the potential are denoted as $A_{l_A,l_B,l}$ and the bispherical harmonics, $I_{l_A,l_B,l}$, are defined as:

$$I_{l_A,l_B,l}(\theta_A,\theta_B,\phi=\phi_A-\phi_B) = \quad (2)$$
$$\sqrt{\frac{2l+1}{4\pi}} \sum_m (l_A\, m\, l_B\, -m|l_A\, l_B\, l\, 0) Y_{l_A,m}(\theta_A,\phi_A) Y_{l_B,-m}(\theta_B,\phi_B),$$

where $Y_{l_i,m}(\theta_i,\phi_i)$ are spherical harmonics and $(l_i\, m\, l_j\, -m|l_i\, l_j\, l\, 0)$ are the Clebsch-Gordan coefficients. In the case of the CO-N_2 system, l_A is a non-negative integer, l_B is a non-negative integer that takes only even values and l satisfies the triangular condition $|l_A - l_B| \leq l \leq l_A + l_B$. Additionally, the sum of these three indices is an even integer.

The radial terms of the potential, $A_{l_A,l_B,l}(R)$, are obtained by the integration of the product of the bispherical harmonics and the full PES, over the angles θ_A, θ_B and ϕ:[124]

$$A_{l_A,l_B,l}(R) = \frac{8\pi^2}{2l+1} \int_0^{2\pi} d\phi \int_0^{\pi} d\theta_A \sin\theta_A \int_0^{\pi} d\theta_B \sin\theta_B \quad (3)$$
$$V(R,\theta_A,\theta_B,\phi) I_{l_A,l_B,l}(\theta_A,\theta_B,\phi)$$

In the cases of Liu's[58] and Surin's[55] PESs, we used their analytical fits. In the case of Cybulski's PES,[57] the reliable fit is limited to energies smaller than 100 μE_h, hence, we interpolated the original 10 000 energy points (which covered the intermolecular distances from 5.0 to 30.0 a_0) with the reproducing kernel Hilbert space method (RKHS).[125] The values of the smoothness parameter, n, and the parameter which determines the long-range behavior of the radial terms, m, were set to the same values as the ones used in the paper of Surin *et al.*[55]

Finally, all the three PESs were prepared in a form of 205 radial terms, up to the term with $l_A = 10$, $l_B = 8$ and $l = 18$. The grid of the intermolecular distances for which the radial terms were calculated, consisted of 230 points, from 4.25 a_0 to 50 a_0. Fig. 2 presents a comparison between isotropic and (two) anisotropic contributions to the three PESs in the vicinity of the minimum of the isotropic component.

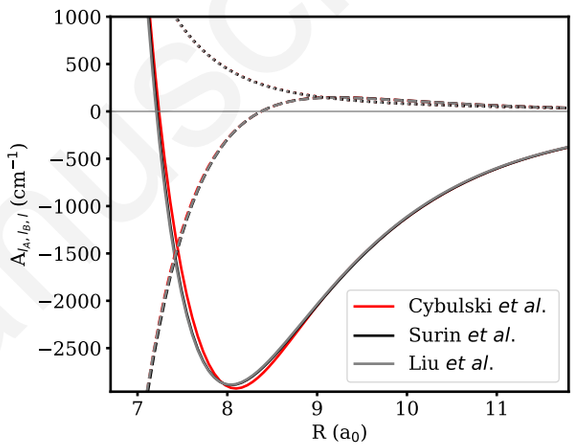

FIG. 2. Comparison between isotropic ($l_A, l_B, l = 0,0,0$, solid lines) and anisotropic ($l_A, l_B, l = 1,0,1$, dashed lines and $l_A, l_B, l = 2,2,4$, dotted lines) radial terms of the three considered PESs.[55,57,58] The two curves corresponding to the isotropic terms of the Surin's and Liu's PES, as well as the curves representing the anisotropic terms for all the three PESs, are overlapping.

III. QUANTUM SCATTERING CALCULATIONS

The quantum scattering theory of two rigid diatomic molecules in a $^1\Sigma$ electronic state is well known and thoroughly discussed in the literature.[124,126–129] Here we briefly summarize the issue and we connect the results of the scattering calculations with the generalized spectroscopic cross section.

The total wavefunction of the system is expanded in a basis set discussed in Ref. 124 or in Ref. 129. The expansion separates the intermolecular distance and the angles describing the geometry of the two diatomics. A substitution of the expanded form of the wavefunction into the Schrödinger equation leads to a set of CC equations for the radial part of the total wavefunction (see Eq. (9) in Ref. 124). The equations are solved numerically for a wide range of kinetic energies. Boundary conditions on the radial part of the total wavefunction connect the solutions of the coupled equations with the

scattering S-matrix (see Eq. (11) of Ref. 128). The elements of the scattering S-matrix enter the formulas for the generalized spectroscopic cross section, whose real and imaginary parts are called the pressure broadening and shift cross section, respectively.[130,131]

In contrast to simpler systems of molecule-atom[107,115,120,132] or molecule-molecule with large rotational constants,[109] for a system of two diatomic molecules typical for Earth's atmosphere, the number of basis levels (necessary to converge numerical calculations) grows considerably with the relative kinetic energy of the colliding pair. At present, this effectively hinders the possibility to study the room-temperature collisions. The memory resources and the CPU time required to perform such calculations exceed capabilities of typical work stations. It has enforced us to use an approximate method of solving the CC equations.

There are several well-known methods for simplifying the coupled equations.[123,133–141] In this work we have made use of the widely used coupled states (CS) approximation.[123] The theory behind the formulas is well-known and the review of the literature can be found in Chapter 9 of Ref. 142.

In the body-fixed frame of reference, the relative angular momentum operator, $\mathbf{l}^2$, couples channels with different values of the projection of the $\mathbf{j}_{12}$ angular momentum, Ω, on the intermolecular axis, where $\mathbf{j}_{12}$ is the result of coupling of the rotational angular momentum of the two diatomic molecules, $\mathbf{j}_{12}=\mathbf{j}_1+\mathbf{j}_2$. Within the most common version of the CS approximation, the off-diagonal matrix elements of the relative angular momentum operator, $\mathbf{l}^2$, coupling different values of Ω, are neglected. This leads to the coupled equations that are diagonal with respect to this quantum number and immensely speeds up the calculations. Additionally, a new quantum number, $\bar{l}$, which approximates the diagonal matrix elements of the relative angular momentum operator as $\bar{l}(\bar{l}+1)$, is introduced. This quantum number is used instead of the total angular momentum, J. Finally, within the CS approximation, the coupled equations are block-diagonal with respect to $\bar{l}$ and Ω.

The rest of the procedure is similar to the case without the approximations. The S-matrix elements (connected with the space-fixed S-matrix elements by a unitary transformation, see Eq. (44) of Ref. 143 and the discussion therein) are obtained and the generalized spectroscopic cross section is calculated. Due to the unitary transformation between the S-matrix elements obtained within the CS approximation and calculated exactly in the space-fixed frame of reference, the formula for the generalized spectroscopic cross section is quite different (see Eq. (96) of Ref. 144):

$$\sigma_0^q(j_i,j_f,j_i',j_f',j_2,E_{\rm kin}) = \tag{4}$$
$$\times\frac{\pi}{k^2}\sqrt{\frac{2j_i'+1}{2j_i+1}}\sum_{\bar{l},\Omega,\Omega'}\sum_{j_2',j_{12},j_{12}',\bar{j}_{12},\bar{j}_{12}'}(-1)^{j_{12}+j_{12}'+\bar{j}_{12}+\bar{j}_{12}'}$$
$$\times(2\bar{l}+1)\sqrt{[j_{12}]\,[j_{12}']\,[\bar{j}_{12}]\,[\bar{j}_{12}']}\begin{pmatrix} j_{12}' & \bar{j}_{12}' & q\\ \Omega & -\Omega' & \Omega'-\Omega\end{pmatrix}$$
$$\times\begin{pmatrix} j_{12} & \bar{j}_{12} & q\\ \Omega & -\Omega' & \Omega'-\Omega\end{pmatrix}\begin{Bmatrix} j_{12}' & \bar{j}_{12}' & q\\ j_i' & j_f' & j_2'\end{Bmatrix}\begin{Bmatrix} j_{12} & \bar{j}_{12} & q\\ j_i & j_f & j_2\end{Bmatrix}$$
$$[\delta_{j_{12}j_{12}'}\delta_{\bar{j}_{12}\bar{j}_{12}'}\delta_{j_ij_i'}\delta_{j_fj_f'}\delta_{j_2j_2'}-$$
$$\langle j_ij_2j_{12}|S^{CS}_{\bar{l}\Omega}(E_{T_i})|j_i'j_2'j_{12}'\rangle\langle j_fj_2\bar{j}_{12}|S^{CS*}_{\bar{l}\Omega'}(E_{T_f})|j_f'j_2'\bar{j}_{12}'\rangle],$$

where $[x]=2x+1$, the quantities in parenthesis are Wigner 3-j symbols and the quantities in braces are Wigner 6-j symbols. If line-mixing effects are not considered, the cross sections are calculated with $j_i=j_i'$ and $j_f=j_f'$, which denote the initial and final states, respectively, of the spectroscopic transition. For the dipole R line analyzed in this work, the tensor order of the radiation-matter interaction, q, is equal to 1.

The results presented here were obtained by solving the coupled equations, within the CS approximation, using MOLSCAT code.[145] The modified log-derivative algorithm of Manolopoulos[146] was used, with propagation beginning deeply in the repulsive wall of the potential at $R=4.25\,a_0$ and ending at $R=100\,a_0$. The radial coupling terms of the PES were extrapolated for $R>50\,a_0$ in a C_n/R^n form, where C_n and n were obtained from the fit using the long range part of the $A_{l_{\rm A},l_{\rm B},l}(R)$ terms. We took advantage of the fact that there are two spin isomers of nitrogen molecule, which give rise to two different symmetries of the rotational wavefunction. *ortho*-N_2, with total nuclear spin $I=0$ or $I=2$, exhibits a rotational structure which involves only even j values, while *para*-N_2, with $I=1$, yields rotational levels which correspond to odd j values. This allowed us to perform scattering calculations with these two species independently, and, thus, to reduce the basis set. At least two asymptotically closed levels ($(j_1;j_2)$ states, the energy of which is larger than the total energy of the scattering system and are thus energetically inaccessible at large intermolecular distances) were kept throughout the calculations. The rotational energy levels of both molecules were taken from HITRAN database.[147] The generalized spectroscopic cross sections were obtained using the newly developed FORTRAN code.[148]

It is difficult to obtain, for a given relative kinetic energy, converged values of the imaginary part of σ_0^1. The pressure shift cross section is very sensitive to the range and step of the propagator and the number of asymptotically closed channels in the basis set (see Sec. 5 of Ref. 115 and Sec. 4 of Ref. 119). The susceptibility of $\mathrm{Im}(\sigma_0^1)$ to these factors is especially pronounced in the molecule-molecule scattering systems and might lead to relatively large uncertainties of the resulting pressure shift coefficients. This is the case for, analyzed here, the N_2-perturbed pure rotational R(0) line in CO. However, the pressure shift is at least two orders of magnitude smaller than the collisional broadening of this particular line and it has not been detected in any experiment.[31,98,99,103]

Thus, in this study, we focus on the real part of σ_0^1 and the resulting pressure broadening coefficient, γ (see Eq. (6)).

We begin the discussion with a comparison of the pressure broadening cross sections obtained using three different PESs. Fig. 3 presents the dependence of σ_0^1 on kinetic energy for $j_2 = 0$. For this particular value of j_2, we were able to calculate the cross sections for the widest range of relative kinetic energies. As it can be seen in Fig. 3, all the three PESs result in almost the same values of the pressure broadening cross sections (the largest relative difference between the cross sections is at a level of 1.5%). The same situation occurs for higher values of j_2, with relative differences between the values of σ_0^1 obtained with different PESs being at the level of 1%. Due to very small differences between the pressure broadening cross sections, in the following analysis we will focus on the results obtained with the PES of Cybulski *et al.*[57]

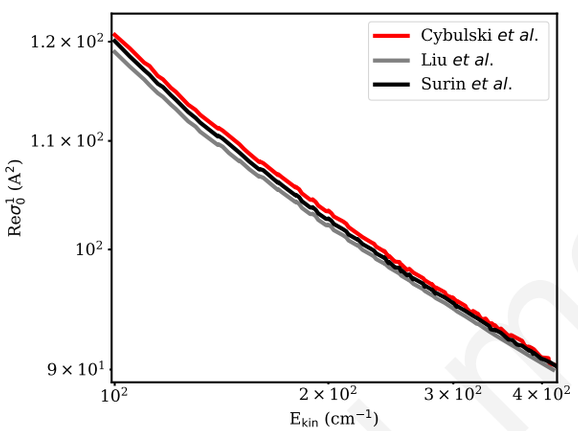

FIG. 3. Comparison between pressure broadening cross sections for $j_2 = 0$ calculated using three different PESs.[55,57,58]

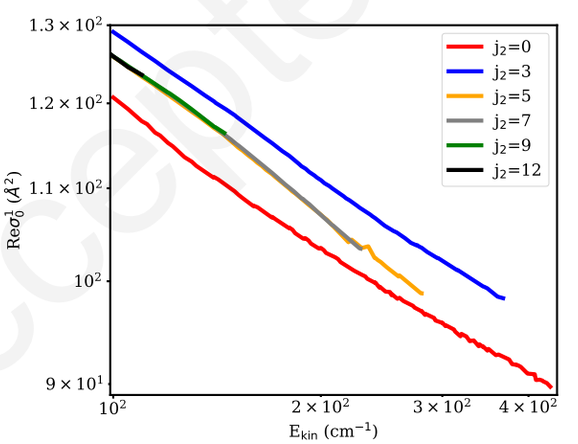

FIG. 4. Pressure broadening cross sections as a function of relative kinetic energy for several values of j_2. The cross sections were calculated using the PES of Cybulski *et al.*[57]

Fig. 4 presents the kinetic energy dependence of the calculated generalized spectroscopic cross sections for various rotational levels of the perturber, j_2. The range of the kinetic energies, for which the calculations of σ_0^1 are feasible, strongly depends on j_2. For example, for $j_2 = 0$, we were able to calculate the cross sections up to kinetic energy values of 400 cm^{-1}, for $j_2 = 7$ up to 250 cm^{-1}, and for $j_2 = 12$ up to 120 cm^{-1}. We note that at large kinetic energies the dependencies are linear on the log-log plot. This type of relation has already been reported in the studies of the argon-perturbed CO lines[122,149,150] as well as in the studies of the Ar-perturbed CO_2[151] or H_2-perturbed N_2[152] isotropic Raman lines. Moreover, it is seen from Fig. 4 that, for a given relative kinetic energy, the pressure broadening cross sections become j_2-independent for larger j_2. A tentative explanation for such behavior of the cross sections is as follows. The PBXS for this system is essentially determined by the contribution from the inelastic state-to-state cross sections (fact that we have checked making use of the random phase approximation[151,153,154]). This is even more evident for larger j_2 values, since the N_2 molecule rotates faster and averages the long range anisotropic components of the PES, resulting in a small elastic dephasing contribution. Therefore, large j_2 values mostly sample the same, short range (repulsive) part of the PES. We thus observe small differences between the PBXS for large j_2 values. This phenomenon was already noticed for several molecule-molecule systems.[152–154] For instance, in the study of C_2H_2-H_2 system,[153] a very weak j_2-dependence of the cross sections for kinetic energies larger than 500 cm^{-1} was reported (see Fig. 3 in Ref. 153 and the discussion therein). In fact, during the calculations of the thermally-averaged pressure broadening coefficient at temperatures larger than 500 K, the cross sections for $j_2 > 3$ were taken as the mean value of σ_0^q with j_2 = 1, 2 and 3. Similar observation about less pronounced j_2-dependence of σ_0^q at large relative kinetic energies were reported in the studies of the N_2-H_2 and N_2-N_2 systems (see Fig. 1 of Ref. 152 and Fig. 3 of Ref. 154, respectively).

The conclusion that $\sigma_0^1(E_{\rm kin})$ obeys the power law allows us to extrapolate it for large kinetic energies. We fit the *ab initio* values of σ_0^1 to the single power law:

$$\sigma_0^1(E_{\rm kin}) = A\left(\frac{E_0}{E_{\rm kin}}\right)^b, \qquad (5)$$

where $E_0 = 100$ cm^{-1}. The cut-off energies are set from 30 to 180 cm^{-1}, depending on the value of j_2. In the case of the extrapolation with respect to the rotational quantum numbers of the perturber, we make use of another observation, that for large values of j_2, for a given kinetic energy, the σ_0^1 cross section converges to a constant value. Thus, we use the following procedure to determine σ_0^1 for given j_2 and $E_{\rm kin}$: for $j_2 < 12$, $\sigma_0^1(E_{\rm kin}, j_2)$ is obtained by fitting the expression given in Eq. (5) to the results of the quantum scattering calculations. For j_2 values larger than 12, we assume that $\sigma_0^1(E_{\rm kin}, j_2) = \sigma_0^1(E_{\rm kin}, j_2 = 12)$.

Figs. 5 and 6 demonstrate the extrapolation procedure for given j_2 and $E_{\rm kin}$, respectively. In Fig. 5, we present the *ab initio* and fitted values of σ_0^1 for $j_2 = 0$ and $j_2 = 7$. As noticed in the previous section, the power-law fit works well at

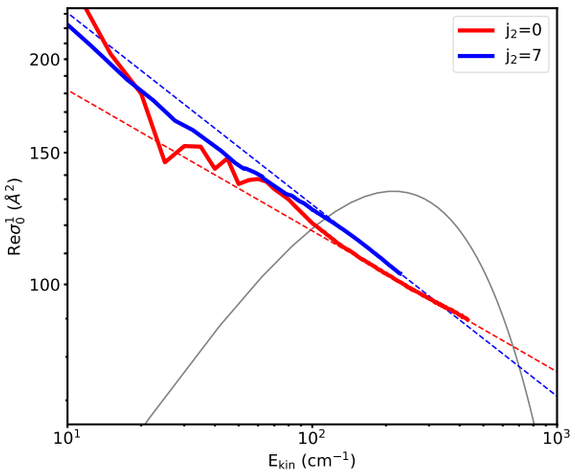

FIG. 5. Kinetic energy dependence of σ_0^1 for $j_2 = 0$ and $j_2 = 7$. The solid and dashed curves correspond to the *ab initio* and fitted (see Eq. (5)) values, respectively. For reference, we put the Maxwell-Boltzmann distribution at 298.15 K (gray curve).

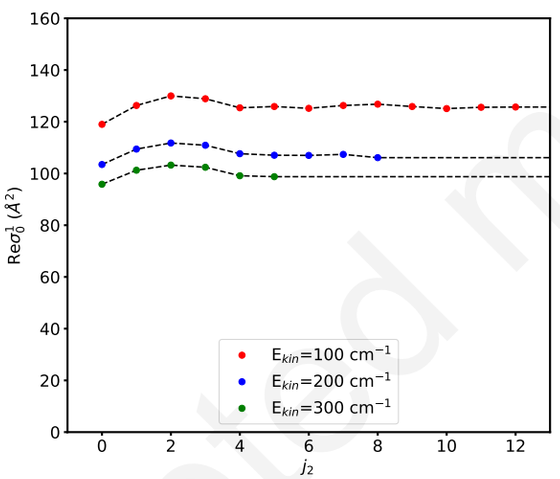

FIG. 6. j_2-dependence of σ_0^1 for various kinetic energies. The points and the black dashed curves correspond to the *ab initio* and the extrapolated values, respectively.

sufficiently large values of $E_{\rm kin}$. In Fig. 6, we show the values of the cross sections as a function of the rotational levels of the perturber, for three kinetic energies: $E_{\rm kin} = 100$, 200 and, 300 cm^{-1}. We note, following the discussion of Fig. 4, that the j_2-dependence of the cross sections becomes less pronounced as j_2 increases. For these three particular values of $E_{\rm kin}$, the cross sections for $j_2 > 5$ differ from each other by less than 0.6%.

In Table I we show the calculated parameters of the power-law fit for $j_2 < 13$ for the three different PESs.[55,57,58] This data can be used to reproduce the shape of the R(0) pure rotational line with different line-shape models (not considered here). Again we can see that the three analyzed PESs lead to almost

TABLE I. Coefficients obtained from the fitted cross section values with the power-law expression, Eq. (5), using three analyzed PESs. Values in parenthesis correspond to the standard deviation error of the parameters.

j_2	Cybulski *et al.*[57]	Surin *et al.*[55]	Liu *et al.*[58]
		A (Å^2)	
0	117.5(1.7)	116.2(1.7)	115.7(2.0)
1	124.7(3.3)	124.3(3.3)	123.7(3.2)
2	127.3(2.4)	127.2(2.1)	127.2(2.2)
3	127.4(3.5)	126.9(4.2)	126.2(3.7)
4	125.4(0.8)	124.8(0.8)	124.3(0.8)
5	125.9(1.0)	125.2(0.7)	124.8(0.7)
6	125.2(0.5)	124.9(0.5)	124.4(0.5)
7	126.3(1.2)	125.9(1.2)	125.5(1.2)
8	126.8(1.2)	126.6(1.2)	125.9(1.4)
9	125.9(1.0)	125.4(1.1)	124.7(1.1)
10	125.1(1.0)	125.0(0.9)	124.4(1.3)
11	125.6(1.9)	125.3(2.2)	125.2(2.4)
12	125.7(2.1)	125.7(2.3)	125.1(3.4)
		b	
0	0.19(2)	0.18(2)	0.18(2)
1	0.19(3)	0.19(3)	0.19(3)
2	0.19(2)	0.19(1)	0.19(2)
3	0.20(3)	0.20(4)	0.20(3)
4	0.22(1)	0.21(1)	0.22(1)
5	0.23(2)	0.23(1)	0.23(1)
6	0.23(1)	0.23(1)	0.23(1)
7	0.24(3)	0.24(3)	0.24(2)
8	0.24(2)	0.24(2)	0.24(3)
9	0.21(2)	0.21(2)	0.21(2)
10	0.21(2)	0.21(2)	0.21(2)
11	0.20(3)	0.21(3)	0.20(3)
12	0.19(4)	0.19(5)	0.19(7)

the same generalized spectroscopic cross sections and that the dependence of the coefficient of the fit on j_2 is negligible for $j_2 > 5$.

IV. LINE-SHAPE PARAMETERS

Generalized spectroscopic cross sections are used to calculate the pressure broadening coefficients at a given temperature T, using the following formula:[109]

$$\gamma(v) = \frac{1}{2\pi c}\frac{1}{k_{\rm B}T}\sum_{j_2} p_{j_2}\frac{2}{\pi \bar{v}_{\rm p} v} \times {\rm Re}\int_0^\infty dv_{\rm r} v_{\rm r}^2 e^{-\frac{v^2+v_{\rm r}^2}{\bar{v}_{\rm p}^2}} \sinh\left(\frac{2vv_{\rm r}}{\bar{v}_{\rm p}^2}\right)\sigma_0^1(j_i, j_f, j_2, v_{\rm r}), \quad (6)$$

where v is the speed of the active molecule, $v_{\rm p}$ denotes the speed of the perturber with the most probable value $\bar{v}_{\rm p} = \sqrt{2k_{\rm B}T/m_{\rm p}}$, and their relative speed $v_{\rm r}$ with the mean value $\bar{v}_{\rm r}$. $m_{\rm p}$ and $k_{\rm B}$ are the mass of the perturber and Boltzmann constant, respectively. p_{j_2} denotes the population of the perturbing molecule in a rotational state j_2 (at a given tempera-

ture):

$$p_{j_2} = \frac{1}{Z(T)} w_{j_2}(2j_2+1)e^{-\frac{E_{j_2}}{k_B T}}, \quad (7)$$

and $Z(T)$ is the partition function

$$Z(T) = \sum_{j_2} w_{j_2}(2j_2+1)e^{-\frac{E_{j_2}}{k_B T}}. \quad (8)$$

In order to cover 99% of the population of the perturber's rotational states at room temperature, one should extend the calculations up to $j_2 = 22$. The weight w_{j_2} comes from the symmetry of the total wavefunction of the nitrogen molecule and the degeneracy of the total nuclear spin, I. The nitrogen nucleus is a boson with the nuclear spin equal 1, which gives the resultant total nuclear spin of the N_2 molecule $I = 0, 1$ or 2. For $I = 0$ and $I = 2$ (*ortho*-N_2), only even values of the rotational quantum number of N_2, j_2, are possible. This corresponds to the value of $w_{j_2} = 6$. *para*-N_2 has the total nuclear spin $I = 1$, with only odd values of j_2 allowed. In this case $w_{j_2} = 3$.

Speed-averaged values of the pressure broadening coefficients (γ_0) are obtained either by averaging Eq. (6) over the velocity distribution of the active molecule or directly from the generalized spectroscopic cross sections:[109]

$$\gamma_0 = \frac{1}{2\pi c}\frac{1}{k_B T}\bar{v}_r \times \sum_{j_2} p_{j_2} \mathrm{Re}\int_0^\infty dx x e^{-x} \sigma_0^q(j_i, j_f, j_2, x = E_{kin}/k_B T). \quad (9)$$

In Fig. 7, we compare the speed-dependent, Eq. (6), and speed-averaged, Eq. (9), values of the pressure broadening coefficient at 298.15 K. We also plot the Maxwellian distribution, which enters Eq. (9) and determines the speed-averaged value of the broadening coefficient.

To compare our calculations with the experimental data, the influence of the speed dependence of the line broadening on the collision-perturbed profile should also be taken into account. The speed dependence of the broadening is manifested as line narrowing, i.e., the effective width of the profile is smaller than γ_0. To account for this effect, we simulated the shape of the line with the weighted sum of Lorentz profiles (WSLP) and fitted the simulated profile with a simple Lorentz profile. The fitted width of the Lorentz profile (denoted here as $\gamma^\dagger$) corresponds to the values that are obtained from the experiments.[31,98,99,103] The influence of the speed dependence of the collisional shift is negligible for this system.

Here, we recall that the line-shape parameters are related to the standard, pressure-dependent broadening coefficients by $\Gamma = \gamma p$, where p denotes the pressure.

V. COMPARISON WITH THE EXPERIMENTAL DATA

In this section, we compare the obtained pressure broadening coefficients with the available experimental data.[31,98,99,103] Connor and Radford[98] reported pressure broadening coefficients for the N_2-, O_2- and air-broadened R(0) lines in CO. The measurements were performed for several temperatures in the range from 202 K to 324 K and the results were fitted to the empirical power law relation:

$$\gamma(T) = C\left(\frac{T_0}{T}\right)^d, \quad (10)$$

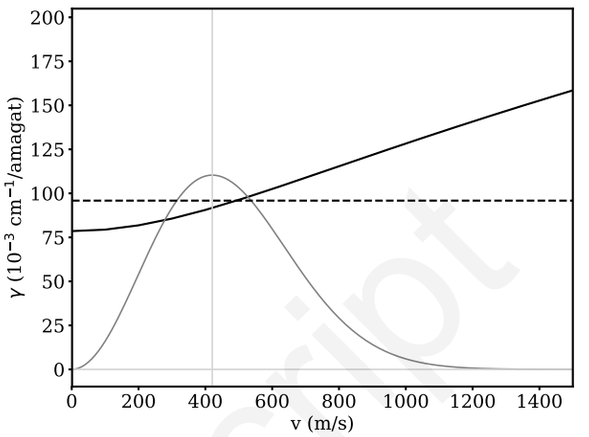

FIG. 7. *Ab initio* speed dependence of the collisional broadening, $\gamma(v)$ (black solid line), for the N_2-perturbed pure rotational R(0) line of the CO molecule at 298.15 K. The speed-averaged value, γ_0, is presented as the black dashed line. For reference, we put the Maxwellian distribution at this temperature (in arbitrary units), as the grey solid curve. The results were obtained using the PES of Cybulski *et al.*[57]

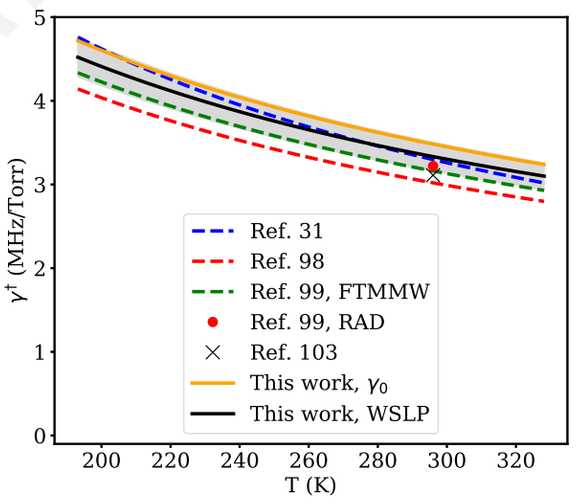

FIG. 8. Comparison between the effective collisional width ($\gamma^\dagger$) of the pure rotational R(0) line of the N_2-perturbed CO molecule with the pressure broadening coefficient (γ_0) and the available experimental data. The estimated uncertainty of $\gamma^\dagger(T)$ is represented by the shaded area (see Sec. VI for details). The results presented here were obtained with the PES of Cybulski *et al.*[57]

TABLE II. Comparison of the theoretical and experimental power law coefficients (Eq. (10)). Dagger symbol, †, denotes the results obtained after the inclusion of the speed-dependence of the broadening (see black curve in Fig. 8). Values in parenthesis correspond to the standard deviation error of the parameters.

PES	C (MHz Torr^{-1})	d
Surin *et al.*[55]	3.44(8)	0.71(14)
Cybulski *et al.*[57]	3.45(7)	0.71(14)
Liu *et al.*[58]	3.43(8)	0.71(14)
Surin *et al.*[55†]	3.29(7)	0.71(14)
Cybulski *et al.*[57†]	3.30(7)	0.71(14)
Liu *et al.*[58†]	3.28(7)	0.71(14)
Experiment (Ref. 31)[a]	3.26(10)	0.86(12)
Experiment (Ref. 98)	2.99(+14,-10)	0.74(10)
Experiment (Ref. 99, FTMMW)	3.13(1)	0.74(2)

[a] The C coefficient is calculated from the C and d values reported for $T_0 = 293$ K.

where $T_0 = 300$ K is a specific reference temperature. The study conducted by Colmont and Monnanteuil[31] was performed in a slightly narrower temperature range, from 220 K to 293 K. The authors derived the values of the fitting coefficients from Eq. (10) for the cases of self-, N_2-, O_2- and air-broadened CO R(0) line, setting $T_0 = 293$ K. Over ten years later, Nissen *et al.*[99] reported results of the joint study conducted by the Kiel and Nizhny Novogrod groups. In this investigation, collisional broadening of the R(0) line in CO by several buffer gases was studied by using two experimental techniques in the time and frequency domain. The frequency-domain data was obtained using radio acoustical detection (RAD) spectrometer for the temperature range from 230 K to 300 K, while the time-domain data was acquired using a Fourier transform spectrometer in the millimeter wave region (FTMMW) at one temperature $T = 296$ K. Puzzarini *et al.*[103] conducted a thorough study of self- and foreign-gas broadening of the R(0-3) lines in the CO (^{12}CO and ^{13}CO) molecules. The authors analyzed the shapes of the measured rovibrational lines using the Voigt, Galatry[155] and Rautian[156] profiles at 296 K.

Fig. 8 presents the comparison between the theoretical and experimental collisional width of the R(0) line of CO perturbed by N_2 at various temperatures. In the case of the theoretical values, we present the speed-averaged pressure broadening coefficient, γ_0, and the effective collisional width of the line, $\gamma^{\dagger}$, as described in Sec. IV. In order to quantitatively compare the theoretical temperature dependence of the collisional width, we chose to present the power law dependence of $\gamma(T)$ by using coefficients fitted with Eq. (10). The theoretical and experimental values of the C and d coefficients are collected in Tab. II.

The agreement between the theoretical and most of the experimental values[31,99,103] is very good. An exception is a slight difference between the theoretical collisional width and the results reported by Connor and Radford.[98] The inclusion of the speed-dependence of collisional broadening through the WSLP leads to significantly better agreement with the experimental data.

VI. ACCURACY OF THE CALCULATIONS

In this section we discuss the sources of the uncertainty of the pressure broadening coefficients reported in this paper. First, we analyze the sources of the uncertainty of the calculated generalized spectroscopic cross sections, originating from the coupled states approximation, the initial parameters of the chosen propagator and the number of the closed levels used in the calculations. In the next step, we discuss the possible error originating from extrapolation of the kinetic energy dependence of the cross sections and, finally, we discuss the influence of neglecting the resonances observed at low kinetic energies. The resulting total uncertainty of the pressure broadening coefficient corresponds to the shaded area in Fig. 8.

The most important contribution to the uncertainty of the final results comes from the coupled states approximation used while solving the coupled equations. The accuracy of the generalized spectroscopic cross sections calculated within this approximation have been thoroughly discussed in the literature.[151,157–159] For instance, Roche *et al.*[157] have reported that for low j values of the active molecule and relatively small values of kinetic energies, the cross sections calculated within the CS approximation are underestimated by about 15%. However, as was confirmed in other studies using this approximation, i.e., in the cases of the molecule-molecule systems, the CS approximation works better in the domain of large kinetic energies and for larger values of j_2.

We have made several tests to check how much the CC and CS generalized spectroscopic cross sections differ. Overall, the agreement between the approximate and exact cross sections is better than previously reported in the literature. The largest relative difference between the CC and CS cross sections in the analyzed energy domain is about 5.8% for $E_{\mathrm{kin}} = 150$ cm^{-1} and $j_2 = 2$. Apart from $j_2 = 0$, where the CS cross sections are underestimated by about 4.5%, the approximate cross sections are slightly larger than the CC values. The largest j_2 value, for which we could make such a comparison was $j_2 = 7$, where we calculated the cross sections for $E_{\mathrm{kin}} = 65$ cm^{-1}. Indeed, the CS works better for larger values of j_2, although we have not observed any sign of convergence of the approximate cross sections to the exact values of σ_0^1. To estimate the error introduced by the CS calculations, we took the relative differences between the CC and CS cross sections from those tests and averaged them with the statistical weights coming from the population of the nitrogen molecule in the considered temperature range. This resulted in an estimated error of 2.7% coming from the approximate method of solving the coupled equations.

Another contribution to the uncertainty of the results originates from the initial parameters of the propagator that is used to solve the coupled equations. Let us remind that we have used the hybrid log-derivative propagator of Manolopoulos,[146] which can be controlled by choosing the starting (R_{min}) and end point (R_{max}) of the propagation, as well as the step size. The choice of the starting point of the propagation is driven by two factors. On the one hand, the propagation process should start possibly deep in the classically forbidden region, where the PES is strongly repulsive.

On the other hand, the quantum chemical methods, such as CCSD(T), are less reliable there since in the short-range region convergence problems tend to occur. This, obviously, affects the accuracy of the radial terms of the PES, that enter the coupled equations. Therefore, one needs to find a starting point which is a compromise between these two restrictions. In this study, we set $R_{\mathrm{min}} = 4.25$ a$_0$, which corresponds to the shortest *ab initio* distance in the R-grid of Surin's PES *et al*.[55] We performed additional tests to check if a decrease in the value of R_{min} to 4.0 a$_0$ or 3.5 a$_0$ has any significant influence on the values of the generalized spectroscopic cross sections. Since the calculated σ_0^1 have remained unchanged in those additional runs, we can state that this parameter is chosen properly.

The propagation should end in the region where the radial terms of the PES vanish and boundary conditions can be applied, and we used $R_{\mathrm{max}} = 100\, a_0$ in our calculations. We have also performed additional tests to check how increasing (up to 200 a_0) or decreasing (down 75 and even 50 a_0) this parameter influences the generalized spectroscopic cross sections. The tests confirmed that increasing this parameter does not produce any significant difference in σ_0^1 and the decrease of this parameter to 50 a_0 affects the pressure broadening cross section by less than 0.01%. We conclude that the range of the propagation has been chosen properly and does not contribute to the final error of the collisional broadening reported here.

A change of the step size of the propagator mainly influences the collisional shift of the spectral line shape, which we do not consider here. Usually, the step size should be inversely proportional to the square root of the relative kinetic energy. However, an appropriate choice of the step size becomes significant for kinetic energies smaller than 40 cm^{-1}, where resonant structures make obtaining the convergence of the cross sections very difficult. In the kinetic energy domain considered here, the error introduced by the step size of the propagator is insignificant.

As mentioned in Sec. III, in all the calculations, we kept at least two asymptotically closed levels. In the considered relative kinetic energy domain this should be sufficient, but we have performed tests to check how additional closed levels (up to 6) influence the values of the pressure broadening cross section. The additional asymptotically closed levels changed the pressure broadening cross section up to about 0.7% of its referential value (for j_2 values larger than 7).

To summarize, the total uncertainty of the calculated pressure broadening cross sections is estimated at a level of 3.5%.

Another important contribution to the uncertainty of the pressure broadening coefficient originates from the extrapolation of the kinetic energy dependence of σ_0^1. Let us remind that for each j_2, the power law function was fitted to the values of σ_0^1. The cut-off energy varied from 30 to 180 cm^{-1}, depending on the j_2 value. In order to estimate the possible error associated with the range of the *ab initio* points used in the fitting procedure, we calculated the pressure broadening coefficients using the power law dependence of $\sigma_0^1(E_{\mathrm{kin}})$ fitted to the data points with $E_{\mathrm{kin}} = 15$ cm^{-1}. The largest relative difference between those values and the results presented here is at a level of 1%.

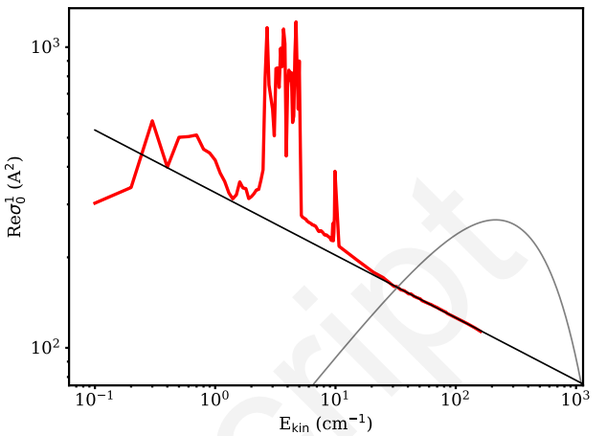

FIG. 9. Resonant structures observed in the pressure broadening cross sections (red curve) for kinetic energies smaller than 15 cm^{-1}. The black line corresponds to the power law function fitted to the points for which $E_{\mathrm{kin}} > 30$ cm^{-1}. As a reference, we draw the Maxwell-Boltzmann distribution at 298.15 K (gray curve). These results, corresponding to $j_2 = 9$, were obtained using the PES of Cybulski *et al*.[57]

In the present study we neglected the resonant structures observed in the kinetic energy dependence of the pressure broadening cross sections. These structures occur for kinetic energies smaller than 15 cm^{-1}, although the exact range depends on j_2. An example for $j_2 = 9$ is presented in Fig. 9. The Maxwell-Boltzmann distribution, shown in this plot, clearly justifies the neglect of the points below 15 cm^{-1} in the calculations of the line-shape parameters (see Eq. (9)) at room temperature. Nonetheless, we have performed tests to quantify the influence of taking into account all the data points, including the resonant structures. We conclude that the results (at room temperature) obtained in this way differ by about 0.5% with respect to the values reported in the previous section.

We have estimated all the possible contributions to the final error of the pressure broadening coefficient. The generalized spectroscopic cross sections are calculated with an approx. 3.5% uncertainty, which originates from the coupled states approximation (2.7%) and the contribution from the number of the closed levels taken into account while solving the coupled equations (0.7%). The cut-offs for the kinetic energies used in the power law fit introduce an estimated error of about 1%. Neglecting the resonant structures of the cross sections for kinetic energies below 10 cm^{-1} could affect the final results by 0.5%. Hence, the total uncertainty of the final pressure broadening coefficients is at the 5% level.

VII. CONCLUSIONS

We have presented the first-ever theoretical calculations of the pressure broadening of the pure rotational R(0) line of the N_2-perturbed CO molecule. Starting from an *ab initio* PES, we performed quantum-scattering calculations. Because

of the computational complexity of the coupled equations, we made use of the well-known coupled states approximation. This allowed us to obtain the generalized spectroscopic cross sections for a wide range of kinetic energies and for the values of the rotational quantum number of the perturbing molecule $j_2 \leq 12$. We calculated the speed-averaged and speed-dependent values of the pressure broadening coefficient and we obtained good agreement with the experimental data.

One of the goals of this paper was to determine whether any of the previously reported PESs[55,57,58] reproduces the shape of the R(0) line significantly better than the other considered PESs. Our results suggest that all three PESs lead to almost the same results and it is impossible, at this level of accuracy of the scattering calculations, to determine which one is the most accurate.

This work constitutes a large step towards theoretical investigation of other N_2-perturbed pure rotational CO lines. Such studies are of particular importance for the physics of the terrestrial and extraterrestrial atmospheres, and for populating the spectroscopic databases, such as the HITRAN database,[147] with *ab initio* collisional line-shape parameters.

SUPPLEMENTARY MATERIAL

See the supplementary material associated with this article for the tabulated radial terms of the three PESs.

ACKNOWLEDGEMENT

H. J. contribution is supported by the National Science Centre in Poland through project no. 2018/31/B/ST2/00720. H. C. contribution was financed by the National Science Centre in Poland within the OPUS 8 project No. 2014/15/B/ST4/04551. P. W. contribution is supported by the National Science Centre in Poland through project no. 2019/35/B/ST2/01118. The project is supported by the French-Polish PHC Polonium program (project 42769ZK for the French part). The project is co-financed by the Polish National Agency for Academic Exchange under the PHC Polonium program (dec. PPN/X/PS/318/2018). The research was part of the program of the National Laboratory FAMO in Toruń, Poland.

DATA AVAILABILITY STATEMENT

The data that supports the findings of this study are available within the article and its supplementary material.

[1] P. E. S. Wormer and A. van der Avoird, "Intermolecular potentials, internal motions, and spectra of van der Waals and hydrogen-bonded complexes," Chem. Rev. **100**, 4109–4144 (2000).

[2] D. Flower, *Molecular collisions in the interstellar medium*, 2nd ed., Cambridge Astrophysics (Cambridge University Press, 2007).

[3] L. Frommhold, *Collision-induced absorption in gases*, Cambridge Monographs on Atomic, Molecular and Chemical Physics (Cambridge University Press, 1994).

[4] J. Hartmann, C. Boulet, and D. Robert, *Collisional Effects on Molecular Spectra* (Elsevier, 2008).

[5] D. L. Hartmann, "Chapter 3 - atmospheric radiative transfer and climate," in *Global Physical Climatology (Second Edition)*, edited by D. L. Hartmann (Elsevier, Boston, 2016) second edition ed., pp. 49 – 94.

[6] J.-M. Hartmann, H. Tran, R. Armante, C. Boulet, A. Campargue, F. Forget, L. Gianfrani, I. Gordon, S. Guerlet, M. Gustafsson, J. T. Hodges, S. Kassi, D. Lisak, F. Thibault, and G. C. Toon, "Recent advances in collisional effects on spectra of molecular gases and their practical consequences," J. Quant. Spectrosc. Radiat. Transf. **213**, 178 – 227 (2018).

[7] D. J. Jacob, *Introduction to atmospheric chemistry* (Princeton University Press, 1999).

[8] A. Eldering, P. O. Wennberg, D. Crisp, D. S. Schimel, M. R. Gunson, A. Chatterjee, J. Liu, F. M. Schwandner, Y. Sun, C. W. O'Dell, C. Frankenberg, T. Taylor, B. Fisher, G. B. Osterman, D. Wunch, J. Hakkarainen, J. Tamminen, and B. Weir, "The orbiting carbon observatory-2 early science investigations of regional carbon dioxide fluxes," Science **358**, eaam5745 (2017).

[9] F. M. Schwandner, M. R. Gunson, C. E. Miller, S. A. Carn, A. Eldering, T. Krings, K. R. Verhulst, D. S. Schimel, H. M. Nguyen, D. Crisp, C. W. O'Dell, G. B. Osterman, L. T. Iraci, and J. R. Podolske, "Spaceborne detection of localized carbon dioxide sources," Science **358**, eaam5782 (2017).

[10] J. C. W. W. W. Carole and N. Beale, *Global climate change linkages: acid rain, air quality, and stratospheric ozone* (Springer Science & Business Media, 1989).

[11] J. S. Daniel and S. Solomon, "On the climate forcing of carbon monoxide," J. Geophys. Res.: Atmospheres **103**, 13249–13260 (1998).

[12] R. D. Stephens and S. H. Cadle, "Remote sensing measurements of carbon monoxide emissions from on-road vehicles," J. Air Waste Manag. Assoc. **41**, 39–46 (1991).

[13] W. W. McMillan, R. B. Pierce, L. C. Sparling, G. Osterman, K. McCann, M. L. Fischer, B. Rappenglück, R. Newsom, D. Turner, C. Kittaka, K. Evans, S. Biraud, B. Lefer, A. Andrews, and S. Oltmans, "An observational and modeling strategy to investigate the impact of remote sources on local air quality: A Houston, Texas, case study from the Second Texas Air Quality Study (TexAQS II)," J. Geophys. Res. **115** (2010), 10.1029/2009jd011973.

[14] C. Shan, W. Wang, C. Liu, Y. Sun, Q. Hu, X. Xu, Y. Tian, H. Zhang, I. Morino, D. W. Griffith, and V. A. Velazco, "Regional CO emission estimated from ground-based remote sensing at Hefei site, China," Atmos. Res. **222**, 25–35 (2019).

[15] D. C. Catling and J. F. Kasting, "Giant planets and their satellites," in *Atmospheric Evolution on Inhabited and Lifeless Worlds* (Cambridge University Press, 2017) p. 393–421.

[16] H. B. Niemann, S. K. Atreya, J. E. Demick, D. Gautier, J. A. Haberman, D. N. Harpold, W. T. Kasprzak, J. I. Lunine, T. C. Owen, and F. Raulin, "Composition of Titan's lower atmosphere and simple surface volatiles as measured by the Cassini-Huygens probe gas chromatograph mass spectrometer experiment," J. Geophys. Res. Planets **115** (2010), 10.1029/2010JE003659.

[17] B. L. Lutz, C. de Bergh, and T. Owen, "Titan: Discovery of carbon monoxide in its atmosphere," Science **220**, 1374–1375 (1983).

[18] F. Flasar, R. Achterberg, B. Conrath, P. Gierasch, V. Kunde, C. Nixon, G. Bjoraker, D. Jennings, P. Romani, A. Simon-Miller, *et al.*, "Titan's atmospheric temperatures, winds, and composition," Science **308**, 975–978 (2005).

[19] R. de Kok, P. Irwin, N. Teanby, E. Lellouch, B. Bézard, S. Vinatier, C. Nixon, L. Fletcher, C. Howett, S. Calcutt, N. Bowles, F. Flasar, and F. Taylor, "Oxygen compounds in Titan's stratosphere as observed by Cassini CIRS," Icarus **186**, 354 – 363 (2007).

[20] D. Muhleman, G. Berge, and R. Clancy, "Microwave measurements of carbon monoxide on Titan," Science **223**, 393–396 (1984).

[21] A. Marten, D. Gautier, L. Tanguy, A. Lecacheux, C. Rosolen, and G. Paubert, "Abundance of carbon monoxide in the stratosphere of Titan from millimeter heterodyne observations," Icarus **76**, 558 – 562 (1988).

[22] M. A. Gurwell and D. O. Muhleman, "CO on Titan: Evidence for a well-mixed vertical profile," Icarus **117**, 375 – 382 (1995).

[23] T. Hidayat, A. Marten, B. Bézard, D. Gautier, T. Owen, H. Matthews, and G. Paubert, "Millimeter and submillimeter heterodyne observations of Titan: The vertical profile of carbon monoxide in its stratosphere," Icarus **133**, 109 – 133 (1998).

[24]M. A. Gurwell and D. O. Muhleman, "CO on Titan: More evidence for a well-mixed vertical profile," Icarus **145**, 653 – 656 (2000).
[25]M. A. Gurwell, "Submillimeter observations of Titan: Global measures of stratospheric temperature, CO, HCN, HC_3N, and the isotopic ratios $^{12}C/^{13}C$ and $^{14}N/^{15}N$," Astrophys. J. **616**, L7–L10 (2004).
[26]K. S. Noll, T. R. Geballe, R. F. Knacke, and Y. J. Pendleton, "Titan's 5 μm spectral window: Carbon monoxide and the albedo of the surface," Icarus **124**, 625 – 631 (1996).
[27]E. Lellouch, A. Coustenis, B. Sebag, J.-G. Cuby, M. López-Valverde, B. Schmitt, T. Fouchet, and J. Crovisier, "Titan's 5-μm window: observations with the Very Large Telescope," Icarus **162**, 125 – 142 (2003).
[28]M. López-Valverde, E. Lellouch, and A. Coustenis, "Carbon monoxide fluorescence from Titan's atmosphere," Icarus **175**, 503 – 521 (2005).
[29]S. M. Hörst, "Titan's atmosphere and climate," J. Geophys. Res. Planets **122**, 432–482 (2017), https://agupubs.onlinelibrary.wiley.com/doi/pdf/10.1002/2016JE005240.
[30]R. Courtin, B. M. Swinyard, R. Moreno, T. Fulton, E. Lellouch, M. Rengel, and P. Hartogh, "First results of Herschel-SPIRE observations of Titan," A&A **536**, L2 (2011).
[31]J. Colmont and N. Monnanteuil, "Self, nitrogen and oxygen broadening of the 115-GHz line of carbon monoxide," J. Quant. Spectrosc. Radiat. Transf. **35**, 81–85 (1986).
[32]N. Semmoud-Monnanteuil and J. Colmont, "Pressure broadening of millimeter lines of carbon monoxide," J. Mol. Spectrosc. **126**, 210–219 (1987).
[33]J.-P. Bouanich, R. Farrenq, and C. Brodbeck, "Direct measurements of N_2 broadened linewidths in the CO fundamental at low temperatures," Can. J. Phys. **61**, 192–197 (1983).
[34]P. Varanasi, S. Chudamani, and S. Kapur, "Diode laser measurements of CO line widths at planetary atmospheric temperatures," J. Quant. Spectrosc. Radiat. Transf. **38**, 167–171 (1987).
[35]A. L. Broadfoot, F. Herbert, J. B. Holberg, D. M. Hunten, S. Kumar, B. R. Sandel, D. E. Shemansky, G. R. Smith, R. V. Yelle, D. F. Strobel, H. W. Moos, T. M. Donahue, S. K. Atreya, J. L. Bertaux, J. E. Blamont, J. C. McConnell, A. J. Dessler, S. Linick, and R. Springer, "Ultraviolet spectrometer observations of Uranus," Science **233**, 74–79 (1986).
[36]Lellouch, E., de Bergh, C., Sicardy, B., Ferron, S., and Käufl, H.-U., "Detection of CO in Triton's atmosphere and the nature of surface-atmosphere interactions," A&A **512**, L8 (2010).
[37]J. L. Elliot, H. B. Hammel, L. H. Wasserman, O. G. Franz, S. W. McDonald, M. J. Person, C. B. Olkin, E. W. Dunham, J. R. Spencer, J. A. Stansberry, M. W. Buie, J. M. Pasachoff, B. A. Babcock, and T. H. McConnochie, "Global warming on Triton," Nature **393**, 765–767 (1998).
[38]L. N. Fletcher, R. Helled, E. Roussos, G. Jones, S. Charnoz, N. André, D. Andrews, M. Bannister, E. Bunce, T. Cavalié, F. Ferri, J. Fortney, D. Grassi, L. Griton, P. Hartogh, R. Hueso, Y. Kaspi, L. Lamy, A. Masters, H. Melin, J. Moses, O. Mousis, N. Nettleman, C. Plainaki, J. Schmidt, A. Simon, G. Tobie, P. Tortora, F. Tosi, and D. Turrini, "Ice giant systems: The scientific potential of orbital missions to Uranus and Neptune," Planet. Space Sci. **191**, 105030 (2020).
[39]S. A. Stern, F. Bagenal, K. Ennico, G. R. Gladstone, W. M. Grundy, W. B. McKinnon, J. M. Moore, C. B. Olkin, J. R. Spencer, H. A. Weaver, L. A. Young, T. Andert, J. Andrews, M. Banks, B. Bauer, J. Bauman, O. S. Barnouin, P. Bedini, K. Beisser, R. A. Beyer, S. Bhaskaran, R. P. Binzel, E. Birath, M. Bird, D. J. Bogan, A. Bowman, V. J. Bray, M. Brozovic, C. Bryan, M. R. Buckley, M. W. Buie, B. J. Buratti, S. S. Bushman, A. Calloway, B. Carcich, A. F. Cheng, S. Conard, C. A. Conrad, J. C. Cook, D. P. Cruikshank, O. S. Custodio, C. M. D. Ore, C. Deboy, Z. J. B. Dischner, P. Dumont, A. M. Earle, H. A. Elliott, J. Ercol, C. M. Ernst, T. Finley, S. H. Flanigan, G. Fountain, M. J. Freeze, T. Greathouse, J. L. Green, Y. Guo, M. Hahn, D. P. Hamilton, S. A. Hamilton, J. Hanley, A. Harch, H. M. Hart, C. B. Hersman, A. Hill, M. E. Hill, D. P. Hinson, M. E. Holdridge, M. Horanyi, A. D. Howard, C. J. A. Howett, C. Jackman, R. A. Jacobson, D. E. Jennings, J. A. Kammer, H. K. Kang, D. E. Kaufmann, P. Kollmann, S. M. Krimigis, D. Kusnierkiewicz, T. R. Lauer, J. E. Lee, K. L. Lindstrom, I. R. Linscott, C. M. Lisse, A. W. Lunsford, V. A. Mallder, N. Martin, D. J. McComas, R. L. McNutt, D. Mehoke, T. Mehoke, E. D. Melin, M. Mutchler, D. Nelson, F. Nimmo, J. I. Nunez, A. Ocampo, W. M. Owen, M. Paetzold, B. Page, A. H. Parker, J. W. Parker, F. Pelletier, J. Peterson, N. Pinkine, M. Piquette, S. B. Porter, S. Protopapa, J. Redfern, H. J. Reitsema, D. C. Reuter, J. H. Roberts, S. J. Robbins, G. Rogers, D. Rose, K. Runyon, K. D. Retherford, M. G. Ryschkewitsch, P. Schenk, E. Schindhelm, B. Sepan, M. R. Showalter, K. N. Singer, M. Soluri, D. Stanbridge, A. J. Steffl, D. F. Strobel, T. Stryk, M. E. Summers, J. R. Szalay, M. Tapley, A. Taylor, H. Taylor, H. B. Throop, C. C. C. Tsang, G. L. Tyler, O. M. Umurhan, A. J. Verbiscer, M. H. Versteeg, M. Vincent, R. Webbert, S. Weidner, G. E. Weigle, O. L. White, K. Whittenburg, B. G. Williams, K. Williams, S. Williams, W. W. Woods, A. M. Zangari, and E. Zirnstein, "The Pluto system: Initial results from its exploration by New Horizons," Science **350**, aad1815–aad1815 (2015).
[40]P. J. Barnes, "A search for CO emission from the Pluto-Charon system," Astron. J. **106**, 2540 (1993).
[41]Bockelée-Morvan, D., Lellouch, E., Biver, N., Paubert, G., Bauer, J., Colom, P., and Lis, D. C., "Search for CO gas in Pluto, Centaurs and Kuiper Belt objects at radio wavelengths," A&A **377**, 343–353 (2001).
[42]J. S. Greaves, C. Helling, and P. Friberg, "Discovery of carbon monoxide in the upper atmosphere of Pluto," Mon. Not. R. Astron. Soc. Lett. **414**, L36–L40 (2011).
[43]E. Lellouch, M. Gurwell, B. Butler, T. Fouchet, P. Lavvas, D. Strobel, B. Sicardy, A. Moullet, R. Moreno, D. Bockelée-Morvan, N. Biver, L. Young, D. Lis, J. Stansberry, A. Stern, H. Weaver, E. Young, X. Zhu, and J. Boissier, "Detection of CO and HCN in Pluto's atmosphere with ALMA," Icarus **286**, 289 – 307 (2017).
[44]L. Young, "Upper limits on gaseous CO at Pluto and Triton from high-resolution near-IR spectroscopy," Icarus **153**, 148–156 (2001).
[45]Lellouch, E., de Bergh, C., Sicardy, B., Käufl, H. U., and Smette, A., "High resolution spectroscopy of Pluto's atmosphere: detection of the 2.3μm CH_4 bands and evidence for carbon monoxide," A&A **530**, L4 (2011).
[46]Y. Xu and A. R. W. McKellar, "Continuous slit-jet infrared spectrum of the CO-N_2 complex," J. Chem. Phys. **104**, 2488–2496 (1996).
[47]Y. Kawashima and K. Nishiza, "Pulsed molecular beam infrared absorption spectroscopy of the N_2-CO complex," Chem. Phys. Lett. **249**, 87 – 91 (1996).
[48]Y. Xu, W. Jäger, L. A. Surin, I. Pak, L. A. Panfilov, and G. Winnewisser, "Microwave and millimeter wave study of *ortho*-N_2 states of CO-N_2," J. Chem. Phys. **111**, 10476–10483 (1999).
[49]Y. Xu and W. Jäger, "The dynamics of the CO-N_2 interaction: Strong coriolis coupling in CO-*para*N_2," J. Chem. Phys. **113**, 514–524 (2000).
[50]L. Surin, H. Müller, E. Alieva, B. Dumesh, G. Winnewisser, and I. Pak, "Detection of the bending vibration of the CO-*ortho*N_2 complex," J. Mol. Struct. **612**, 207 – 211 (2002).
[51]L. Surin, A. Potapov, H. Müller, V. Panfilov, B. Dumesh, T. Giesen, and S. Schlemmer, "Millimeter-wave study of the CO-N_2 van der Waals complex: new measurements of CO-*ortho*N_2 and assignments of new states of CO-*para*N_2," J. Mol. Struct. **795**, 198 – 208 (2006).
[52]L. Surin, A. Potapov, H. Müller, and S. Schlemmer, "A new millimeter-wave observation of the weakly bound CO-N_2 complex," J. Mol. Spectrosc. **307**, 54–58 (2015).
[53]C. Xia, A. R. W. McKellar, and Y. Xu, "Infrared spectrum of the CO-N_2 van der Waals complex: Assignments for CO-*para*-N_2 and observation of a bending state for CO-*ortho*-N_2," J. Chem. Phys. **113**, 525–533 (2000).
[54]M. Rezaei, K. H. Michaelian, N. Moazzen-Ahmadi, and A. R. W. McKellar, "A new look at the infrared spectrum of the weakly bound CO-N_2 complex," J. Phys. Chem. A **117**, 13752–13758 (2013).
[55]L. A. Surin, I. V. Tarabukin, S. Schlemmer, Y. N. Kalugina, and A. van der Avoird, "*Ab initio* potential and rotational spectra of the CO-N_2 complex," J. Chem. Phys. **148**, 044313 (2018).
[56]I. Tarabukin, L. Surin, and S. Schlemmer, "Millimeter-wave detection of doubly excited bending mode in the CO–N_2 van der Waals complex," J. Mol. Spectrosc. **362**, 21–24 (2019).
[57]H. Cybulski, C. Henriksen, R. Dawes, X.-G. Wang, N. Bora, G. Avila, T. Carrington Jr., and B. Fernández, "*Ab initio* study of the CO-N_2 complex: a new highly accurate intermolecular potential energy surface and rovibrational spectrum," Phys. Chem. Chem. Phys. **20**, 12624–12636 (2018).
[58]J.-M. Liu, Y. Zhai, X.-L. Zhang, and H. Li, "Intermolecular configurations dominated by quadrupole-quadrupole electrostatic interactions: explicit correlation treatment of the five-dimensional potential energy surface and infrared spectra for the CO-N_2 complex," Phys. Chem. Chem. Phys.

20, 2036 (2018).
[59]J. Fiser and R. Polák, "An ab initio study of the CO-N_2 complex," Chem. Phys. Lett. **360**, 565 – 572 (2002).
[60]M. H. Karimi-Jafari, A. Maghari, and A. Farjamnia, "Intermolecular potential energy surface of the N_2-CO dimer: Ab initio investigation and analytical representation," J. Phys. Chem. A **115**, 1143–1151 (2011).
[61]D. R. Eaton and H. W. Thompson, "Pressure broadening studies on vibration-rotation bands II. The effective collision diameters," Proc. Roy. Soc. London Ser. A **251**, 475–485 (1959).
[62]C. Crane-Robinson and H. W. Thompson, "Pressure broadening studies on vibration-rotation bands. IV. Optical collision diameters for foreign-gas broadening of CO and DCl bands," Proc. Roy. Soc. London Ser. A **272**, 453–466 (1963).
[63]A.-T. Chai and D. Williams, "Comparison of collision cross sections for line broadening in the CO fundamental," J. Opt. Soc. Am. **58**, 1395 (1968).
[64]D. Williams, D. C. Wenstrand, R. J. Brockman, and B. Curnutte, "Collisional broadening of infra-red absorption lines," Mol. Phys. **20**, 769–785 (1971).
[65]J.-P. Bouanich and C. Haeusler, "Linewidths of carbon monoxide self-broadening and broadened by argon and nitrogen," J. Quant. Spectrosc. Radiat. Transf. **12**, 695–702 (1972).
[66]P. Varanasi and S. Sarangi, "Measurements of intensities and nitrogen-broadened linewidths in the CO fundamental at low temperatures," J. Quant. Spectrosc. Radiat. Transf. **15**, 473–482 (1975).
[67]P. Varghese and R. Hanson, "Tunable infrared diode laser measurements of line strengths and collision widths of $^{12}C^{16}O$ at room temperature," J. Quant. Spectrosc. Radiat. Transf. **24**, 479–489 (1980).
[68]J. A. Sell, "Temperature dependence of the absorption coefficient and halfwidth of the P(6) line of carbon monoxide," J. Quant. Spectrosc. Radiat. Transf. **23**, 595–598 (1980).
[69]J. N.-P. Sun and P. R. Griffiths, "Nitrogen-broadening coefficient of vibration–rotation lines of carbon monoxide," Appl. Opt. **20**, 2332 (1981).
[70]H. S. Lowry and C. J. Fisher, "Line parameter measurements and calculations of CO broadened by nitrogen at elevated temperatures," J. Quant. Spectrosc. Radiat. Transf. **27**, 585–591 (1982).
[71]T. Nakazawa and M. Tanaka, "Measurements of intensities and self- and foreign-gas-broadened half-widths of spectral lines in the CO fundamental band," J. Quant. Spectrosc. Radiat. Transf. **28**, 409–416 (1982).
[72]T. Nakazawa and M. Tanaka, "Intensities, half-widths and shapes of spectral lines in the fundamental band of CO at low temperatures," J. Quant. Spectrosc. Radiat. Transf. **28**, 471–480 (1982).
[73]M. Bulanin, A. Dokuchaev, M. Tonkov, and N. Filippov, "Influence of line interference on the vibration-rotation band shapes," J. Quant. Spectrosc. Radiat. Transf. **31**, 521–543 (1984).
[74]J. Bonamy, D. Robert, and C. Boulet, "Simplified models for the temperature dependence of linewidths at elevated temperatures and applications to CO broadened by Ar and N_2," J. Quant. Spectrosc. Radiat. Transf. **31**, 23–34 (1984).
[75]M. Moal and F. Severin, "N_2 and H_2 broadening parameters in the fundamental band of CO," J. Quant. Spectrosc. Radiat. Transf. **35**, 145–152 (1986).
[76]J. Hartmann, M. Perrin, J. Taine, and L. Rosenmann, "Diode-laser measurements and calculations of CO 1-0 P(4) line broadening in the 294- to 765-K temperature range," J. Quant. Spectrosc. Radiat. Transf. **35**, 357–363 (1986).
[77]J.-P. Bouanich and G. Blanquet, "Pressure broadening of CO and OCS spectral lines," J. Quant. Spectrosc. Radiat. Transf. **40**, 205–220 (1988).
[78]A. Hamdouni, A. Barbe, J.-J. Plateaux, V. Langlois, V. Dana, J.-Y. Mandin, and M. Badaoui, "Measurements of N_2-induced shifts and broadening coefficients of lines in CO fundamental from Fourier transform spectra," J. Quant. Spectrosc. Radiat. Transf. **50**, 247–255 (1993).
[79]N. Anselm, K. Yamada, R. Schieder, and G. Winnewisser, "Measurements of foreign gas pressure shift and broadening effects in the (1-0) band of CO with N_2 and Ar," J. Mol. Spectrosc. **161**, 284–296 (1993).
[80]P. Duggan, P. M. Sinclair, M. P. Le Flohic, J. W. Forsman, R. Berman, A. D. May, and J. R. Drummond, "Testing the validity of the optical diffusion coefficient: Line-shape measurements of CO perturbed by N_2," Phys. Rev. A **48**, 2077–2083 (1993).
[81]J. Mandin, V. Dana, M. Badaoui, A. Barbe, A. Hamdouni, and J. Plateaux, "Measurements of pressure-broadening and pressure-shifting coefficients from FT spectra," J. Mol. Spectrosc. **164**, 328–337 (1994).
[82]P. Duggan, P. M. Sinclair, A. D. May, and J. R. Drummond, "Line-shape analysis of speed-dependent collisional width inhomogeneities in CO broadened by Xe, N_2, and He," Phys. Rev. A **51**, 218–224 (1995).
[83]A. Henry, D. Hurtmans, M. Margottin-Maclou, and A. Valentin, "Confinement narrowing and absorber speed dependent broadening effects on CO lines in the fundamental band perturbed by Xe, Ar, Ne, He and N_2," J. Quant. Spectrosc. Radiat. Transf. **56**, 647–671 (1996).
[84]J.-P. Bouanich, D. Bermejo, J. Domenech, R. Martinez, and J. Santos, "Pressure-induced lineshifts in the $2 \leftarrow 0$ band of CO self-perturbed and perturbed by He, Kr, O_2, and N_2," J. Mol. Spectrosc. **179**, 22–31 (1996).
[85]P. Sinclair, P. Duggan, R. Berman, A. May, and J. Drummond, "Line broadening, shifting, and mixing in the fundamental band of CO perturbed by N_2 at 301 K," J. Mol. Spectrosc. **181**, 41–47 (1997).
[86]B. Sumpf, J. Burrows, A. Kissel, H.-D. Kronfeldt, O. Kurtz, I. Meusel, J. Orphal, and S. Voigt, "Line shift investigations for different isotopomers of carbon monoxide," J. Mol. Spectrosc. **190**, 226–231 (1998).
[87]T. Drascher, T. Giesen, T. Wang, N. Schmücker, R. Schieder, G. Winnewisser, P. Joubert, and J. Bonamy, "Temperature-dependent line shift and broadening of CO infrared transitions," J. Mol. Spectrosc. **192**, 268–276 (1998).
[88]A. Predoi-Cross, C. Luo, P. Sinclair, J. Drummond, and A. May, "Line broadening and the temperature exponent of the fundamental band in CO–N_2 mixtures," J. Mol. Spectrosc. **198**, 291 – 303 (1999).
[89]M. Afzelius, P.-E. Bengtsson, and J. Bonamy, "Semiclassical calculations of collision line broadening in Raman spectra of N_2 and CO mixtures," J. Chem. Phys. **120**, 8616–8623 (2004).
[90]T. C. James and E. K. Plyler, "Linewidths in the 2–0 band of carbon monoxide broadened by nitrogen and hydrogen," J. Chem. Phys. **40**, 221–223 (1964).
[91]J.-P. Bouanich and C. Brodbeck, "Mesure des largeurs et des deplacements des raies de la bande $0 \rightarrow 2$ de CO autoperturbé et perturbé par N_2, O_2, H_2, HCl, NO et CO_2," J. Quant. Spectrosc. Radiat. Transf. **13**, 1–7 (1973).
[92]J.-P. Bouanich, "Lineshifts in the first overtone band of CO self-perturbed and perturbed by N_2 at 298, 193, and 133 K," Can. J. Phys. **61**, 919–922 (1983).
[93]S. Voigt, S. Dreher, J. Orphal, and J. P. Burrows, "N_2-broadening in the $^{13}C^{16}O$ 2–0 band around 4167 cm^{-1}," J. Mol. Spectrosc. **180**, 359–364 (1996).
[94]A. Predoi-Cross, J. P. Bouanich, D. C. Benner, A. D. May, and J. R. Drummond, "Broadening, shifting, and line asymmetries in the $2 \leftarrow 0$ band of CO and CO–N_2: Experimental results and theoretical calculations," J. Chem. Phys. **113**, 158–168 (2000).
[95]D. E. Burch and D. A. Gryvnak, "Strengths, widths, and shapes of the lines of the 3ν CO band," J. Chem. Phys. **47**, 4930–4940 (1967).
[96]J. Henningsen, H. Simonsen, T. Møgelberg, and E. Trudsø, "The $0 \rightarrow 3$ overtone band of CO: Precise linestrengths and broadening parameters," J. Mol. Spectrosc. **193**, 354–362 (1999).
[97]A. Predoi-Cross, C. Hnatovsky, K. Strong, J. Drummond, and D. C. Benner, "Temperature dependence of self- and N_2-broadening and pressure-induced shifts in the $3 \leftarrow 0$ band of CO," J. Mol. Struct. **695-696**, 269–286 (2004).
[98]B. J. Connor and H. Radford, "Pressure broadening of the CO J = 1-0 rotational transition by N_2, O_2, and air," J. Mol. Spectrosc. **119**, 229 – 231 (1986).
[99]N. Nissen, J. Doose, A. Guarnieri, H. Mäder, V. N. Markov, G. Y. Golubyatnikov, I. Leonov, V. N. Shanin, and A. F. Krupnov, "Foreign gas broadening studies of the $J' \rightarrow J = 1 \rightarrow 0$ rotational line of CO by frequency and time domain techniques," Z. Naturforsch A **54**, 218 – 224 (1999).
[100]D. Priem, F. Rohart, J.-M. Colmont, G. Wlodarczak, and J.-P. Bouanich, "Lineshape study of the $J=3 \leftarrow 2$ rotational transition of CO perturbed by N_2 and O_2," J. Mol. Struct. **517-518**, 435 – 454 (2000).
[101]V. Markov, G. Golubiatnikov, V. Savin, D. Sergeev, A. Guarnieri, and H. Mäder, "Line broadening and shifting studies of the $J=5 \leftarrow 4$ transition of carbon monoxide perturbed by CO, N_2, and O_2," J. Mol. Spectrosc. **212**, 1 – 5 (2002).
[102]J.-M. Colmont, L. Nguyen, F. Rohart, and G. Wlodarczak, "Lineshape analysis of the $J=3 \leftarrow 2$ and $J=5 \leftarrow 4$ rotational transitions of room temperature CO broadened by N_2, O_2, CO_2 and noble gases," J. Mol. Spectrosc. **246**, 86–97 (2007).

[103]C. Puzzarini, L. Dore, and G. Cazzoli, "A comparison of lineshape models in the analysis of modulated and natural rotational line profiles: Application to the pressure broadening of OCS and CO," J. Mol. Spectrosc. **216**, 428–436 (2002).

[104]P. S. Hsu, H. U. Stauffer, N. Jiang, J. R. Gord, and S. Roy, "Direct measurements of collisional Raman line broadening in the S-branch transitions of CO perturbed by CO, N_2, and CO_2," Appl. Opt. **58**, C1–C6 (2019).

[105]M. Słowiński, F. Thibault, Y. Tan, J. Wang, A.-W. Liu, S.-M. Hu, S. Kassi, A. Campargue, M. Konefał, H. Jóźwiak, K. Patkowski, P. Żuchowski, R. Ciuryło, D. Lisak, and P. Wcisło, "H_2-He collisions: Ab initio theory meets cavity-enhanced spectra," Phys. Rev. A **101**, 052705 (2020).

[106]B. W. Bakr, D. G. A. Smith, and K. Patkowski, "Highly accurate potential energy surface for the He–H_2 dimer," J. Chem. Phys. **139**, 144305 (2013).

[107]F. Thibault, K. Patkowski, P. S. Żuchowski, H. Jóźwiak, R. Ciuryło, and P. Wcisło, "Rovibrational line-shape parameters for H_2 in He and new H_2-He potential energy surface," J. Quant. Spectrosc. Radiat. Transf. **202**, 308 – 320 (2017).

[108]R. Blackmore, "A modified Boltzmann kinetic equation for line shape functions," J. Chem. Phys. **87**, 791–800 (1987).

[109]P. Wcisło, F. Thibault, M. Zaborowski, S. Wójtewicz, A. Cygan, G. Kowzan, P. Masłowski, J. Komasa, M. Puchalski, K. Pachucki, R. Ciuryło, and D. Lisak, "Accurate deuterium spectroscopy for fundamental studies," J. Quant. Spectrosc. Radiat. Transf. **213**, 41 – 51 (2018).

[110]R. Ciuryło, D. A. Shapiro, J. R. Drummond, and A. D. May, "Solving the line-shape problem with speed-dependent broadening and shifting and with Dicke narrowing. II. Application," Phys. Rev. A **65**, 012502 (2001).

[111]A. May, W.-K. Liu, F. McCourt, R. Ciuryło, J. S.-F. Stoker, D. Shapiro, and R. Wehr, "The impact theory of spectral line shapes: a paradigm shift," Can. J. Phys. **91**, 879–895 (2013).

[112]P. R. Berman, "Speed-dependent collisional width and shift parameters in spectral profiles," J. Quant. Spectrosc. Radiat. Transf. **12**, 1331–1342 (1972).

[113]R. H. Dicke, "The effect of collisions upon the Doppler width of spectral lines," Phys. Rev. **89**, 472–473 (1953).

[114]F. Thibault, P. Wcisło, and R. Ciuryło, "A test of H_2-He potential energy surfaces," Eur. Phys. J. D **70**, 236 (2016).

[115]H. Jóźwiak, F. Thibault, N. Stolarczyk, and P. Wcisło, "Ab initio line-shape calculations for the S and O branches of H_2 perturbed by He," J. Quant. Spectrosc. Radiat. Transf. **219**, 313 – 322 (2018).

[116]M. Słowiński *et al.*, in preparation.

[117]P. Wcisło, F. Thibault, N. Stolarczyk, H. Jóźwiak, M. Słowinski, M. Gancewski, K. Stankiewicz, M. Konefał, S. Kassi, A. Campargue, Y. Tan, J. Wang, K. Patkowski, R. Ciuryło, D. Lisak, R. Kochanov, L. Rothman, and I. Gordon, "The first comprehensive dataset of beyond-Voigt line-shape parameters from ab initio quantum scattering calculations for the HITRAN database: He-perturbed H_2 case study," J. Quant. Spectrosc. Radiat. Transf. **260**, 107477 (2021).

[118]F. Thibault, R. Z. Martínez, D. Bermejo, and P. Wcisło, "Line-shape parameters for the first rotational lines of HD in He," Mol. Astroph. **19**, 100063 (2020).

[119]K. Stankiewicz, H. Jóźwiak, M. Gancewski, N. Stolarczyk, F. Thibault, and P. Wcisło, "Ab initio calculations of collisional line–shape parameters and generalized spectroscopic cross-sections for rovibrational dipole lines in HD perturbed by He," J. Quant. Spectrosc. Radiat. Transf. **254**, 107194 (2020).

[120]R. Z. Martínez, D. Bermejo, F. Thibault, and P. Wcisło, "Testing the ab initio quantum-scattering calculations for the D_2-He benchmark system with stimulated Raman spectroscopy," J. Raman Spectrosc. **49**, 1339–1349 (2018).

[121]R. Z. Martínez, D. Bermejo, P. Wcisło, and F. Thibault, "Accurate wavenumber measurements for the $S_0(0)$, $S_0(1)$, and $S_0(2)$ pure rotational Raman lines of D_2," J. Raman Spectrosc. **50**, 127–129 (2018).

[122]G. Kowzan, H. Cybulski, P. Wcisło, M. Słowiński, A. Viel, P. Masłowski, and F. Thibault, "Subpercent agreement between ab initio and experimental collision-induced line shapes of carbon monoxide perturbed by argon," Phys. Rev. A **102**, 012821 (2020).

[123]P. McGuire and D. J. Kouri, "Quantum mechanical close coupling approach to molecular collisions. j_z-conserving coupled states approximation," J. Chem. Phys. **60**, 2488–2499 (1974).

[124]S. Green, "Rotational excitation in H_2-H_2 collisions: Close-coupling calculations," J. Chem. Phys. **62**, 2271–2277 (1975).

[125]T.-S. Ho and H. Rabitz, "Proper construction of ab initio global potential surfaces with accurate long-range interactions," J. Chem. Phys. **113**, 3960–3968 (2000).

[126]G. Gioumousis and C. F. Curtiss, "Molecular collisions. II. Diatomic molecules," J. Math. Phys. **2**, 96–104 (1961).

[127]W. D. Davison, "Rotational energy transfer in molecular collisions: transitions in *para*-hydrogen," Discuss. Faraday Soc. **33**, 71–84 (1962).

[128]H. Klar, "Theory of scattering between two rigid rotors," Z. Phys. **228**, 59 (1969).

[129]M. H. Alexander and A. E. DePristo, "Symmetry considerations in the quantum treatment of collisions between two diatomic molecules," J. Chem. Phys. **66**, 2166–2172 (1977).

[130]L. Monchick and L. W. Hunter, "Diatomic-diatomic molecular collision integrals for pressure broadening and Dicke narrowing: A generalization of Hess's theory," J. Chem. Phys. **85**, 713–718 (1986).

[131]J. Schaefer and L. Monchick, "Line shape cross sections of HD immersed in He and H_2 gas. I. Pressure broadening cross sections," J. Chem. Phys. **87**, 171–181 (1987).

[132]P. Wcisło, F. Thibault, H. Cybulski, and R. Ciuryło, "Strong competition between velocity-changing and phase- or state-changing collisions in H_2 spectra perturbed by Ar," Phys. Rev. A **91**, 052505 (2015).

[133]T. P. Tsien and R. T. Pack, "Rotational excitation in molecular collisions: A strong coupling approximation," Chem. Phys. Lett. **6**, 54 – 56 (1970).

[134]T. P. Tsien and R. T. Pack, "Rotational excitation in molecular collisions. Corrections to a strong coupling approximation," Chem. Phys. Lett. **6**, 400 – 402 (1970).

[135]T. Tsien and R. Pack, "Rotational excitation in molecular collisions. A many-state test of the strong coupling approximation," Chem. Phys. Lett. **8**, 579 – 581 (1971).

[136]R. Pack, "Relations between some exponential approximations in rotationally inelastic molecular collisions," Chem. Phys. Lett. **14**, 393 – 395 (1972).

[137]H. Rabitz, "Effective potentials in molecular collisions," J. Chem. Phys. **57**, 1718–1725 (1972).

[138]A. E. DePristo and M. H. Alexander, "A decoupled l-dominant approximation for ion-molecule and atom-molecule collisions," J. Chem. Phys. **64**, 3009–3013 (1976).

[139]A. E. DePristo and M. H. Alexander, "Limits of validity of the decoupled l-dominant approximation," Chem. Phys. Lett. **44**, 214 – 218 (1976).

[140]A. E. DePristo and M. H. Alexander, "Decoupling approximations for rotationally inelastic collisions between ions and polar molecules: H^+-CN," J. Phys. B-At. Mol. Opt. **9**, 2713–2721 (1976).

[141]R. Goldflam, S. Green, and D. J. Kouri, "Infinite order sudden approximation for rotational energy transfer in gaseous mixtures," J. Chem. Phys. **67**, 4149–4161 (1977).

[142]D. G. Truhlar, J. T. Muckerman, and R. Bernstein, "Atom-molecule collision theory: A guide for the experimentalist," by RB Bernstein, Plenum Press, London , 505 (1979).

[143]D. J. Kouri, T. G. Heil, and Y. Shimoni, "On the Lippmann-Schwinger equation for atom-diatom collisions: A rotating frame treatment," J. Chem. Phys. **65**, 226–235 (1976).

[144]R. Goldflam and D. J. Kouri, "On angular momentum decoupling approximations and factorization in diatom-diatom scattering," J. Chem. Phys. **70**, 5076–5091 (1979).

[145]J. Hutson and S. Green, "Molscat computer code, version 14," Collaborative computational project (1994).

[146]D. E. Manolopoulos, "An improved log derivative method for inelastic scattering," J. Chem. Phys. **85**, 6425–6429 (1986).

[147]I. Gordon, L. Rothman, C. Hill, R. Kochanov, Y. Tan, P. Bernath, M. Birk, V. Boudon, A. Campargue, K. Chance, B. Drouin, J.-M. Flaud, R. Gamache, J. Hodges, D. Jacquemart, V. Perevalov, A. Perrin, K. Shine, M.-A. Smith, J. Tennyson, G. Toon, H. Tran, V. Tyuterev, A. Barbe, A. Császár, V. Devi, T. Furtenbacher, J. Harrison, J.-M. Hartmann, A. Jolly, T. Johnson, T. Karman, I. Kleiner, A. Kyuberis, J. Loos, O. Lyulin, S. Massie, S. Mikhailenko, N. Moazzen-Ahmadi, H. Müller, O. Naumenko, A. Nikitin, O. Polyansky, M. Rey, M. Rotger, S. Sharpe, K. Sung, E. Starikova, S. Tashkun, J. V. Auwera, G. Wagner, J. Wilzewski, P. Wcisło, S. Yu, and E. Zak, "The HITRAN2016 molecular spectroscopic

database," J. Quant. Spectrosc. Radiat. Transf. **203**, 3 – 69 (2017), HITRAN2016 Special Issue.

[148]F. Thibault, "Pressure broadening and shift code for 2 diatomics - coupled states approximation," Mendeley Data, V1 (2020), http://dx.doi.org/10.17632/ykxz36nwry.1.

[149]R. Wehr, A. Vitcu, R. Ciuryło, F. Thibault, J. R. Drummond, and A. D. May, "Spectral line shape of the $P(2)$ transition in CO-Ar: Uncorrelated ab initio calculation," Phys. Rev. A **66**, 062502 (2002).

[150]G. Kowzan, P. Wcisło, M. Słowiński, P. Masłowski, A. Viel, and F. Thibault, "Fully quantum calculations of the line-shape parameters for the Hartmann-Tran profile: A CO-Ar case study," J. Quant. Spectrosc. Radiat. Transf. **243**, 106803 (2020).

[151]F. Thibault, B. Calil, J. Buldyreva, M. Chrysos, J.-M. Hartmann, and J.-P. Bouanich, "Experimental and theoretical CO_2-Ar pressure-broadening cross sections and their temperature dependence," Phys. Chem. Chem. Phys. **3**, 3924–3933 (2001).

[152]L. Gomez, S. V. Ivanov, O. G. Buzykin, and F. Thibault, "Comparison of quantum, semiclassical and classical methods in hydrogen broadening of nitrogen lines," J. Quant. Spectrosc. Radiat. Transf. **112**, 1942 – 1949 (2011).

[153]F. Thibault, B. Corretja, A. Viel, D. Bermejo, R. Z. Martinez, and B. Bussery-Honvault, "Linewidths of C_2H_2 perturbed by H_2: experiments and calculations from an ab initio potential," Phys. Chem. Chem. Phys. **10**, 5419–5428 (2008).

[154]F. Thibault, R. Z. Martinez, D. Bermejo, and L. Gómez, "Collisional line widths of autoperturbed N_2: Measurements and quantum calculations," J. Quant. Spectrosc. Radiat. Transf. **112**, 2542 – 2551 (2011).

[155]L. Galatry, "Simultaneous effect of Doppler and foreign gas broadening on spectral lines," Phys. Rev. **122**, 1218–1223 (1961).

[156]S. G. Rautian and I. I. Sobelman, "The effect of collisions on the Doppler broadening of spectral lines-," Soviet Physics Uspekhi **9**, 701–716 (1967).

[157]C. F. Roche, A. S. Dickinson, and J. M. Hutson, "A failing of coupled-states calculations for inelastic and pressure-broadening cross sections: Calculations on CO_2-Ar," J. Chem. Phys. **111**, 5824–5828 (1999).

[158]F. Thibault, R. Z. Martinez, J. L. Domenech, D. Bermejo, and J.-P. Bouanich, "Raman and infrared linewidths of CO in Ar," J. Chem. Phys. **117**, 2523–2531 (2002).

[159]R. Z. Martinez, J. L. Domenech, D. Bermejo, F. Thibault, J.-P. Bouanich, and C. Boulet, "Close coupling calculations for rotational relaxation of CO in Argon: Accuracy of energy corrected sudden scaling procedures and comparison with experimental data," J. Chem. Phys. **119**, 10563–10574 (2003).